New Carbazole-Based Sensitizers for p-Type DSSCs: Impact of the Position of Acceptor Units on Device Performance

Kavya Keremane, Yann Pellegrin, Aurélien Planchat, Denis Jacquemin, Fabrice Odobel, Airody Vasudeva Adhikari

New Carbazole-Based Sensitizers for *p*-Type DSSCs: Impact of the Position of Acceptor Units on Device Performance

Kavya S. Keremane[a], Yann Pellegrin[b], Aurélien Planchat[b], Denis Jacquemin[b]*, Fabrice Odobel[b,]*, and Airody Vasudeva Adhikari[a,c,]*

[a] Organic Materials Laboratory, Department of Chemistry, National Institute of Technology Karnataka, Surathkal, Mangalore-575025, India

[b] Nantes Université, CNRS, CEISAM UMR 6230, Nantes, France.

[c] Yenepoya Research Centre, Yenepoya deemed to be University, Deralakatte, Mangalore-575 018, India

*Corresponding authors e-mail: *denis.jacquemin@univ-nantes.fr* (Denis Jacquemin), *fabrice.odobel@univ-nantes.fr* (Fabrice Odobel), *avachem@gmail.com* (A. Vasudeva Adhikari)

Abstract

We report the design, synthesis, and characterization of two new carbazole-based organic dyes **PC1-2** as potential sensitizers for NiO-based *p*-type dye-sensitized solar cells (*p*-DSSCs). The D-A-π-A configured **PC1** dye comprises a thienyl unit as a π-spacer and a malononitrile as an end-capping acceptor unit, whereas in **PC2** the cyanovinylene group serves as an acceptor unit and a thienyl group acts as a donor unit in a D-A-D configuration. These molecules achieved excellent solubility due to their long-branched alkyl chains. The current work encompasses their structural, photophysical, thermal, electrochemical, theoretical, and photoelectrochemical studies allowing establishing of structure-property relationships. **PC1-2** exhibit λ_{abs} and λ_{emi} in the range of 389-404 nm and 448-515 nm, respectively, with a bandgap in the order, 2.88-2.92 eV. Electrochemical studies confirm the feasibility of electron injection, regeneration, and recombination. The introduction of an additional electron withdrawing group (cyanovinylene group) on the dye **PC1** skeleton endows with a higher dye loading capacity, high hole injection, and a strengthened ICT effect, resulting in a red-shifted ICT absorption with a higher molar extinction coefficient. Among the two new dyes, the device based on **PC1** achieved the highest power conversion efficiency (*PCE*) of 0.027% with short-circuit current density (J_{SC}) of 1.29 mA·cm^{-2}, open-circuit voltage (V_{OC}) of 67 mV, and fill factor (*FF*) of 31%, whereas the device with dye **PC2** performed less efficiently (*PCE*: 0.018 %, J_{SC}: 0.92 mA·cm^{-2}, V_{OC}: 68 mV, and *FF*: 30 %). Conclusively, the study provides insights into the intricacies involved in the structural modification of carbazole-based *p*-type dyads for the development of highly efficient DSSCs.

Keywords: DSSC; sensitizers; donor-acceptor; carbazole; time-dependent density functional theory

Introduction

As an emerging photovoltaic technology, dye-sensitized solar cells (DSSCs) have attracted greater attention due to their valuable features such as low cost, design versatility, facile fabrication process, efficiency, and eco-friendly nature.[1-3] To date, the majority of the DSSC efforts have been devoted to improving the photovoltaic performance of *n*-type DSSCs.[4-5] Nevertheless, their efficiency is still lagging behind when compared to that of traditional silicon solar cells, which hampered large-scale commercial applications.[6-8] *p*-type dye-sensitized solar cells (*p*-DSSC), based on sensitization of *p*-type semiconductor such as NiO, are gaining increased interest as this complementary photoanode provides an alternative path to improve the use of solar energy. [9-10] One of the main purposes of developing *p*-type DSSCs is to combine them with *n*-type DSSCs to fabricate tandem solar cells and improve the power conversion efficiency (*PCE*).[11-13] As per the Shockley-Queisser limitation, the highest theoretical limit of efficiency for the single solar cell is about 33 %, whereas the *p*-*n* tandem devices carrying two photoactive semiconductors can have overall *PCE* as high as 43%.[14] Moreover, such photocathodes can be used in Dye-Sensitized Photoelectrosynthesis Cell (DSPEC) for solar fuel production.[20-21] Currently, the poor performance of *p*-type materials limits the efficiency of solar cells and DSPECs and hence there is a demand for the development of more efficient sensitizers.[15-19] In *p*-type DSSCs, among all the other components, sensitizers, used as light harvesters play a pivotal role in capturing photons leading first to a photoexcited state that is followed by a decay to the ground state thanks to hole injection into the valence band (VB) of the NiO semiconductor.[10,22] A specific strategy to improve the performance of *p*-DSSCs is to introduce an organic dye with the "push-pull" configuration, which significantly enhances the light-harvesting capacity and hole injection capability leading to an optimal photoinduced intramolecular charge transfer (ICT), dragging the electron far from the surface.[23-25] Besides, D-π-A configured *p*-type sensitizer helps to limit the hole recombination between NiO photocathode and the electrolytes or reduced dye, resulting in increased photocurrent density.[18]

During the past two decades, numerous organic chromophores have been introduced to achieve the requirements of efficient *p*-type sensitizers. For instance, dyes based on

triphenylamine, coumarin, perylene, squaraine, and porphyrin chromogens have been used as *p*-type sensitizers in NiO-based DSSCs.[22,26-28] Carbazole derivatives are widely applied in optoelectronic and photovoltaic applications owing to their excellent charge-transporting properties, easy synthesis, tuneable absorption properties, electrochemical stability, and high molar extinction coefficient.[29-30] Besides, their HOMO-LUMO energy levels can be easily tuned through functionalization at different positions, rendering them potential candidates for *p*-type sensitizer. In addition, the *N*-heteroatom of the carbazole ring can be straightforwardly substituted with various functional groups to further promote charge separation as well as to limit aggregation.[31] Further, the introduction of a linker unit between the donor and acceptor moieties allows tuning both the optical and charge transport properties. Thiophene is one of the most extensively studied linker in *n*-type DSSCs due to their high polarizability, molar absorptivity, stability, and excellent charge transporting capability.[32] The presence of thiophene spacer not only extends the π-conjugation of the dye but also enhances its overall stability.[33-34] Furthermore, the incorporation of cyanovinylene group as an auxiliary acceptor unit very next to the electron donors is a smooth approach to further enhance the π-conjugation and induce bathochromic and hyperchromic shifts of the absorption band. It also moves the electron density away from the surface and retards charge recombination.[35-37] The position and number of acceptor units play a pivotal role in determining the overall performance of the solar cells. However, in terms of carbazole-based *p*-type DSSCs, the studies are limited.[31]

In the present work, we synthesized two new carbazole-based organic chromophores with the two different design strategies and investigated how the presence of auxiliary acceptor units as well as end-capping acceptor units impacts the performances of the solar cells (**Figure 1**). The newly designed molecules were synthesized from simple starting material 9*H*-carbazole following a multistep synthesis pathway (**Scheme 1**). These dyes show excellent solubility due to the presence of long-branched alkyl chains. The schematic representation of design strategies/chemical structures of new *p*-type dyes **PC$_{1\text{-}2}$** along with benchmark reference dye **P1** is shown in **Figure 1**. Here, the design strategy of D-A-π-A' configured dye **PC$_1$** involves carbazole moiety as an electron donor, cyanovinylene as an second electron acceptor unit, thiophene moiety as a spacer, malononitrile as an electron acceptor, and carboxylic acid as an anchoring unit, whereas in **PC$_2$** carbazole as well as thiophene moieties act as an electron donor and the cyanovinylene group serves as an auxiliary acceptor unit in a D-A-π-A' architecture. This molecular design proved to be

particularly suitable to develop better performing sensitizers, since the photovoltaic performances of **PC$_1$** are higher than that of **PC$_2$**. However, the specific mode of binding by both carboxylic acid and cyano groups certainly force the dyes to lay down on NiO surface and promotes charge recombination.

All target dyes and their corresponding intermediates were fully characterized using ^{1}H NMR, ^{13}C NMR, FT-IR, mass spectroscopy, and elemental analyses. Their photophysical, as well as electrochemical properties, were examined by means of UV-Visible absorption, photoluminescence (PL), and cyclic voltammetric (CV) studies. Also, their thermal behaviour was evaluated by thermogravimetric analysis (TGA) studies. Furthermore, the molecular geometry and absorption spectra were theoretically investigated using time-dependent density functional theory (TD-DFT). Finally, the synthesized dyes were employed as sensitizers in NiO-based *p*-type DSSCs and their photovoltaic performance data were measured. Quantum efficiency measurements were carried out to determine their incident photon to current conversion efficiency (*IPCE*) spectra.

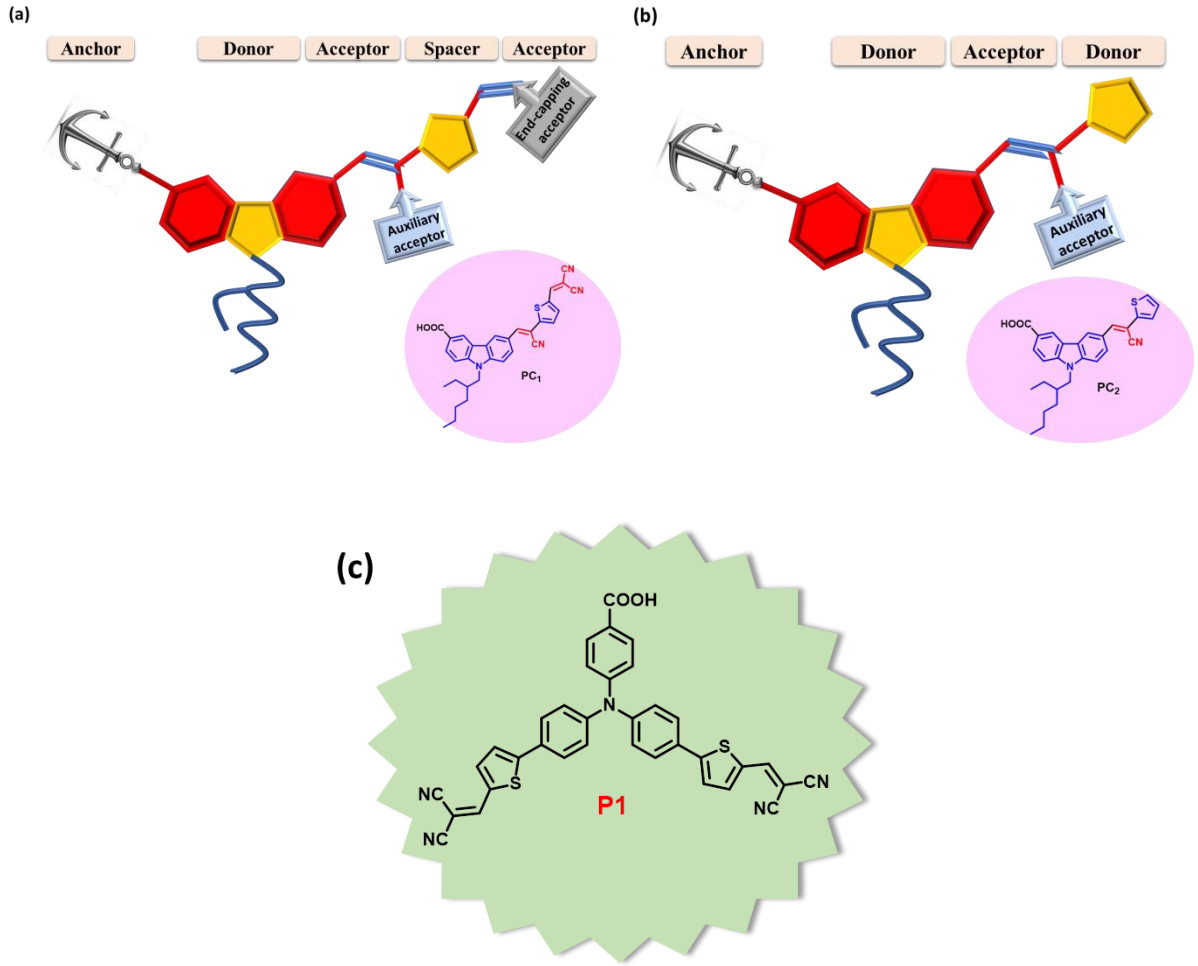

Figure 1. Schematic representation of design strategies of new organic chromophores (**a**) **PC1**, (**b**) **PC2**, and (**c**) chemical structure of benchmark reference dye **P1**.

Results and discussion

Synthesis and characterization

The synthetic pathways of new carbazole-based organic sensitizers (**PC1-2**) are depicted in **Scheme 1**. The requested intermediate 9-(2-ethylhexyl)-9*H*-carbazole (**1**) was obtained from starting material 9*H*-carbazole by treating it with 2-ethylhexyl bromide in the presence of sodium hydride. This was converted to the key precursor intermediate 9-(2-ethylhexyl)-9*H*-carbazole-3-carbaldehyde (**2)** *via* Vilsmeier-Haack reaction. The intermediate **2** was oxidized to get 9-(2-ethylhexyl)-9*H*-carbazole-3-carboxylic acid (**3**) with Ag_2O as an oxidising agent. Then, the carboxylic group of the **3** was protected by esterification (Fisher ester synthesis) to give **4**. Further, the ester **4** was formylated using the Vilsmeier-Haack reaction protocol to get methyl 9-(2-ethylhexyl)-6-formyl-9*H*-carbazole-3-carboxylate (**5)**. Afterwards, **5** was further condensed with thiophene-2-acetonitrile by the Knoevenagel condensation to obtain *(Z)*-methyl 6-(2-cyano-2-(thiophen-2-yl)vinyl)-9-(2-ethylhexyl)-9*H*-carbazole-3-carboxylate (**6**). Furthermore, **6** was formylated using the Vilsmeier-Hack reaction protocol and the crude product (**7**) was hydrolyzed with lithium hydroxide to deliver intermediate **8**. In the final step, the target molecule **PC1** was obtained in good yield by following the Knoevenagel condensation of (*Z*)-6-(2-cyano-2-(5-formylthiophen-2-yl)vinyl)-9-(2-ethylhexyl)-9*H*-carbazole-3-carboxylic acid (**8**) with an active methylene compound, *viz.* malononitrile, whereas **PC2** was obtained by hydrolysis of (*Z*)-methyl 6-(2-cyano-2-(thiophen-2-yl)vinyl)-9-(2-ethylhexyl)-9*H*-carbazole-3-carboxylate (**6**). The detailed synthetic procedures of all the intermediates, as well as target molecules, are given in the SI. All the synthesized compounds were purified using recrystallization or column chromatography techniques. The molecular structures of the newly synthesized dyes and their intermediates were confirmed by using various spectroscopy methods (**S1-S14**, ESI) and elemental analysis.

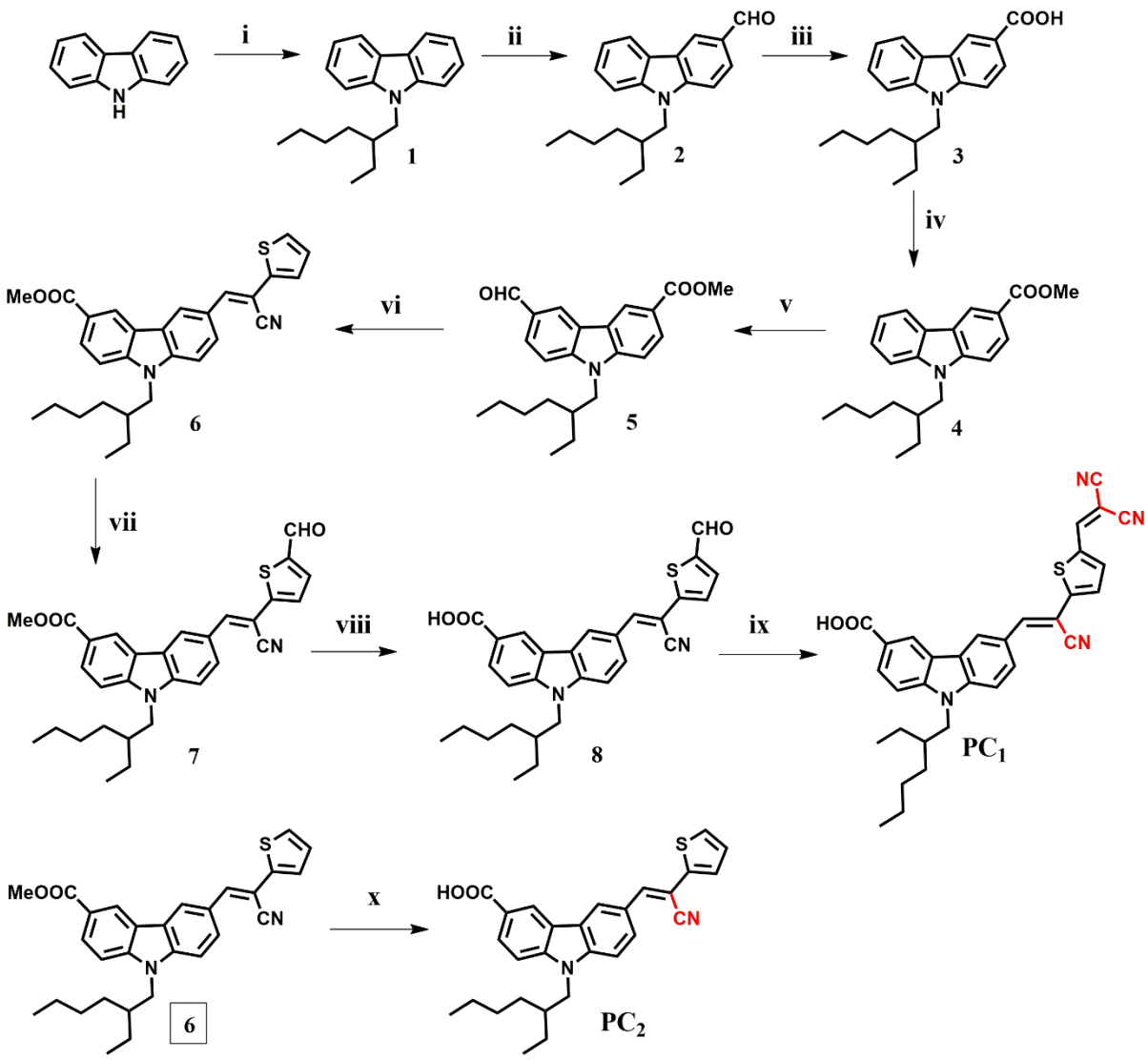

Scheme 1. Synthetic routes for the dyes **PC1-2**: (i) 2-Ethylhexyl bromide, NaH, DMF, RT, 12 h, 92 %; (ii) $POCl_3$, DMF, RT, 12 h, 69 %; (iii) Ag_2O, NaOH, EtOH, RT, 12 h, 72 %; (iv) MeOH, H_2SO_4, reflux, 88 %; (v) DMF, $POCl_3$, 90 ºC, 12h, 52 %; (vi) Thiophene-2-acetonitrile, Na metal, MeOH, RT, 24 h, 80 %; (vii) DMF, $POCl_3$, 90 ºC, 12h, 64 %; (viii) $LiOH.H_2O$, MeOH, 80 ºC, 12 h, 59 %; (ix) **PC1**: malononitrile, DMF, 90 ºC, 12 h, 82 %; (x) **PC2**: $LiOH.H_2O$, MeOH, 80 ºC, 12 h, 85 %.

Theoretical studies

Theoretical calculations were next performed to obtain insights into the photophysical features of the new dyes. The methods are detailed in the SI,[38] but we stress that we use a range-separated hybrid functional for modelling the optical spectrum, as ICT is expected to occur in these compounds. Results are summarized in **Table 1**. Theory returns bright low-lying transitions at 466 nm (f=1.37) for **PC1** and 376 nm (f=1.30) for **PC2**. There is a clear

redshift in **PC$_1$** as compared to **PC$_2$**. For comparison, the same level of theory gives 453 nm (*f*=1.12) for **P1**. More interesting density difference plots are shown in **Figure 2**. In **PC$_1$** there is a clear ICT character, the carbazole acting as the donor, the malononitrile as the acceptor, and the thienyl and the bridging unit. The ICT is computed to transfer 0.56 electrons over 3.33 Å (see **Table 1**), which are quite large values, indicating significant electron-hole separation. Interestingly, one notes that the cyanovinylene group of **PC$_1$** is simply a bridge, the cyano group being passive in the excitation process. The situation is different in **PC$_2$**: the thienyl and carbazole act as donating moieties (mostly in blue) and the cyanovinylene is the main acceptor. In such a D-A-D configuration, the ICT is significantly smaller (0.50 electron over 1.28 Å). As can be seen in **Table 1**, both the ground and excited-state dipoles of **PC$_2$** are also much smaller than their **PC$_1$** counterparts. For comparison, we have provided the same density difference plots for the **P1** dye. While the overall CT is similar to the one of **PC$_1$** (0.69 electron over 2.89 Å), one clearly sees in **Figure 2** that the anchoring group of **P1** undergoes a drop of density, a favorable effect when grafted on the surface as it helps hole injection, whereas in both the synthesized dyes, the ICT process takes place further away from the anchoring unit, which is not ideal.

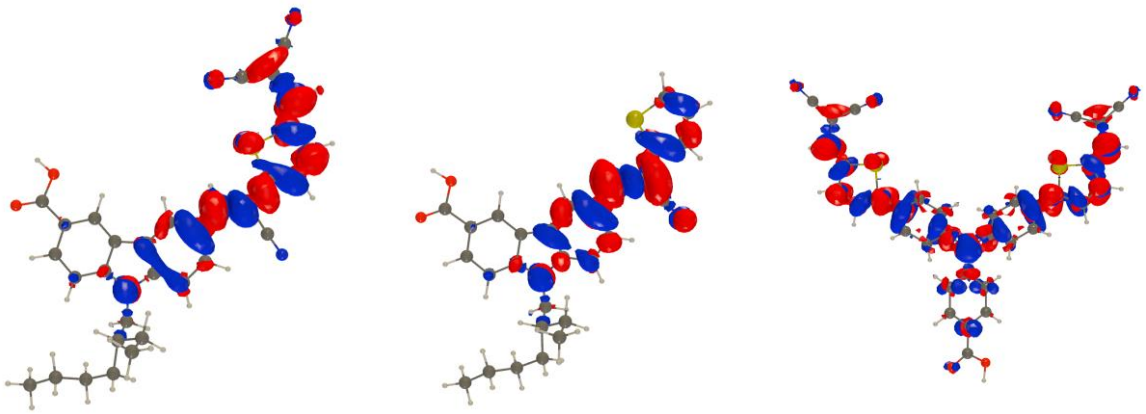

PC$_1$ **PC$_2$** **P1**

Figure 2. Electron density difference (EDD) plots (contour 1x10^{-3}) for the two synthesized dyes **PC$_{1-2}$** as compared to reference dye **P1**. The red and blue regions are corresponding to zones of increase and decrease of electronic density upon photoexcitation, respectively.

Table 1. TD-DFT determined data for **PC1-2** along with reference dye **P1**. The data includes the vertical absorption, related oscillator strength, the ICT parameters (ICT distance and amount of charge transferred), as well as the computed ground and excited state dipole moments.

Compound	λ_{vert} (nm)	*f*	$E_{0\text{-}0}$ (eV)	d^{CT}_i (Å)	q^{CT}_i (e)	μ_{GS} (D)	μ_{ES} (D)
PC1	466	1.37	2.44	3.33	0.56	11.4	19.3
PC2	376	1.30	2.98	1.28	0.50	1.7	4.7
P1	453	1.12	2.53	2.89	0.67	19.9	29.3

Optical properties

The UV-Vis absorption spectra of the new *p*-type organic chromophores **PC1-2** are measured in 10^{-5} M DMF solutions and are depicted in **Figure 3a** whereas the key spectral data are summarized in **Table 2**. The newly synthesized **PC1** shows two distinctive absorption bands. The absorption band in the region of 310-340 nm can be assigned to the π-π* electronic excitations localized within the carbazole donor, whereas the peak corresponding to the longer wavelength, *i.e.*, 380-410 nm can be attributed to the ICT from the donor to the electron acceptor unit, consistent with the TD-DFT analysis. Likewise, the dye **PC2** displays a single weak ICT absorption peak which is less intense and blue-shifted *vs.* **PC1**. It is therefore clear that **PC1** possesses a broader, more intense, and redshifted absorption band than **PC2**, for reasons explained above. The aforesaid shift is quite desirable as it shows an improved light-harvesting ability in the devices. In addition, the molar extinction coefficients (**ε**) of all the molecules **PC1-2** were determined according to the Lambert-Beer law (see the SI).[39-40] The **ε** values are rather large for both dyes, *i.e.*, **PC1** (22900 $M^{-1}cm^{-1}$) > **PC2** (13100 $M^{-1}cm^{-1}$), confirming superior light-harvesting ability of **PC1**.

Further, the normalized emission spectra of **PC1-2** are measured in 10^{-5} M DMF solutions (**Figure 3b** and **Table 2**). The fluorescence emission spectra display a single emission band at 515 nm (**PC1**) and 448 nm (**PC2**) with a larger Stokes shift for **PC1** (5330 cm^{-1}) than **PC2** (3380 cm^{-1}). The zero-zero excited state energy ($E_{0\text{-}0}$) between the ground

state and the first singlet excited of **PC1** and **PC2** are calculated to be 2.92 and 2.88 eV, respectively[41] (**Table 2**).

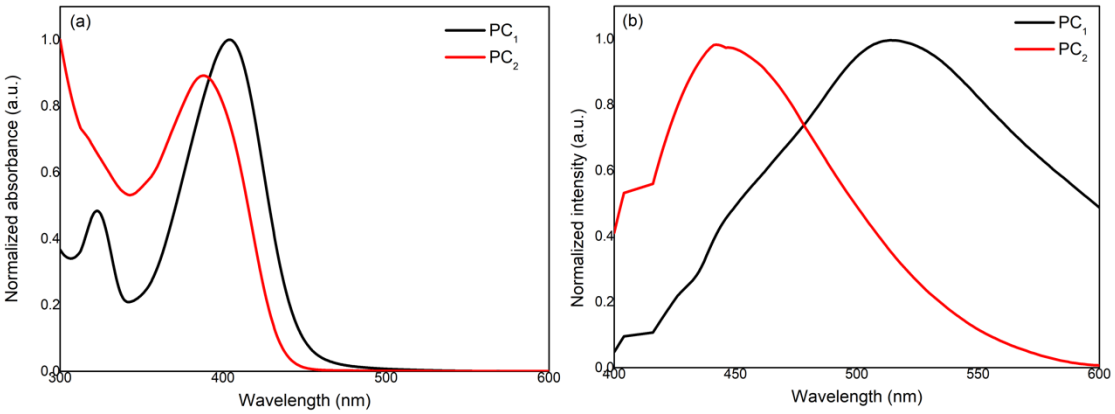

Figure 3. (a) UV-Vis absorption and (**b**) corrected fluorescence spectra of **PC1-2** recorded in DMF solution; excitation wavelength at the maximum absorption wavelength of **PC1** and **PC2**.

Table 2. Photophysical properties of **PC1-2** recorded in DMF at room temperature.

Compound	**λ_{abs}[a] (nm)**	**λ_{emi}[a] (nm)**	**Stokes shift (cm^{-1})**	**ε ($M^{-1}cm^{-1}$) at λ_{abs} (nm)**	**$E_{0\text{-}0}$[b] opt (eV)**
PC1	404	515	5330	22 900	2.92
PC2	389	448	3380	13 100	2.88

[a] Emission spectra measured in DMF at optical density of 0.1 on the maximum absorption wavelength.[b] Optical band gap $E_{0\text{-}0}$ is the energy measured vertically at the intersection point between normalized absorption and emission spectra.

Finally, to elucidate the mode of binding of the dyes on NiO surface, the attenuated total reflection infrared (ATR-IR) spectra of the sensitizers after their chemisorption on NiO and compare them to the bare dye (Figure S10 and S14). In KBr pallet, the stretching band of carbonyl group of dye **PC1** and **PC2** and appears respectively at 1680 cm^{-1} and 1599 cm^{-1} while that of the cyano group are located at 2222 cm^{-1} and 2208 cm^{-1} respectively. After chemisorption on NiO, the carbonyl band is broadened and shifted to higher wavenumber, witnessing the coordination bond established with nickel oxide. Moreover, the intensity of the stretching band of cyano unit is decreased and also broadened suggesting an interaction of cyano group with NiO surface as well. Consequently, the attachment of these dyes by both carboxylic acid and cyano groups certainly forces the dyes to lay horizontally on NiO surface.

Thermal properties

The thermal characteristics of the dyes **PC1-2** were studied by thermogravimetric analyses (TGA) at the heating rate of 10 °C min^{-1} under a nitrogen atmosphere. The TGA plots of **PC1-2** are shown in **Figure 4**. The synthesized dyes exhibit satisfactory thermal stability with high thermal decomposition (T_d) temperatures at 347 °C (**PC1**) and 314 °C (**PC2**), and consequently, their application as sensitizers would result in good stability of the devices.

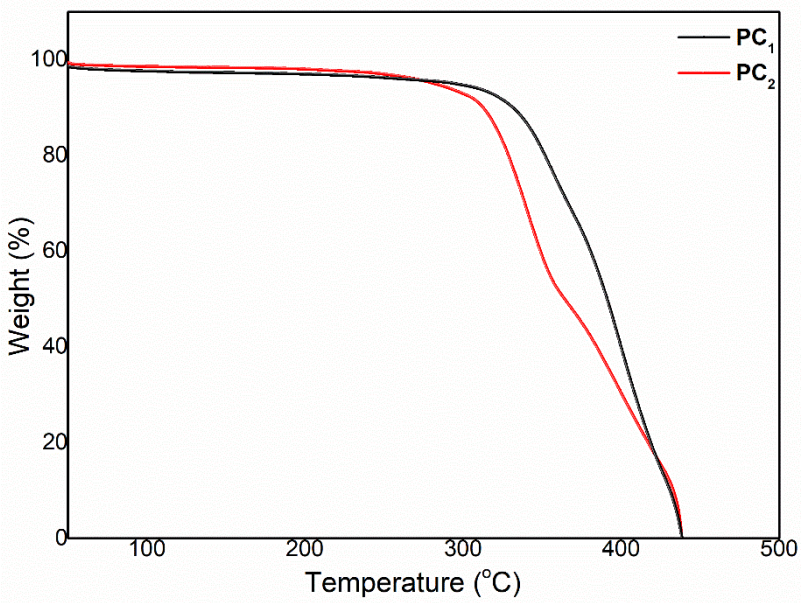

Figure 4. TGA thermograms of **PC1-2** obtained at heating rate of 10 °C min^{-1} under nitrogen atmosphere

Electrochemical properties

The feasibility of thermodynamically allowed hole injection from the excited dye molecules into the VB of NiO and subsequent electron transfer from the (photo)reduced dye to the redox couple in the electrolyte can be determined using redox potentials and $E_{0\text{-}0}$.[42] The cyclic voltammetry (CV) experiments were performed and the generated voltammograms of **PC1-2** are depicted in **Figure S15**. In the CV experiments, the cyclic voltammograms were recorded between +2 and –2 V, and the deduced energy level diagram is given in **Figure S16**.

To investigate the thermodynamic feasibility of hole injection and dye regeneration processes of **PC1-2**, the free energies (ΔG_{inj} and ΔG_{reg}) were estimated using Eqs. (1) and (2),[43] the corresponding data being listed in **Table 3**. The energy levels were efficiently tuned

by varying electron acceptor units, indicating a significant influence on both the hole injection and dye regeneration efficiencies. The Gibbs free energy to inject charge from the highest occupied level of the dye to the VB edge of the NiO semiconductor was estimated according to Eq(1).

$$\Delta G_{\mathrm{inj}} = E_{\mathrm{VB}}(NiO) - E^{*}_{\mathrm{Red}} \,, \qquad (1)$$

with ΔG_{inj} the free energy for injection, E^{*}_{red} the reduction potential of the dye and E_{VB} (NiO) the Nernst potential of the VB of NiO, *i.e.*, 0.30 V *vs.* SCE. Furthermore, the Gibbs energy for dye regeneration from electrolyte (ΔG_{reg}) was estimated from the difference between the reduction potential of the dye and Nernst potential of I_3^-/I^- electrolyte system (-0.32 V) using,

$$\Delta G_{\mathrm{reg}} = E_{\mathrm{Red}} - E_{I_3^-/I_2^{-\cdot}} \,. \qquad (2)$$

The ΔG_{inj} values are very large for both dyes (around –1.8 eV), meaning that these dyes are suitable for p-SCs with even high valence band potential, whereas the ΔG_{reg} values are much lower (around –0.4 eV) and similar for both dyes but sufficient to guarantee efficient regeneration. In short, the electrochemical studies revealed that all the *p*-type organic chromophores (**PC1-2**) fulfilled the prerequisites for effective electron injection and dye regeneration processes in the fabricated devices.

Table 3. Electrochemical properties of *p*-type organic chromophores **PC1-2**

Compound	E_{red} (V)	E_{red}^{*} (V)	ΔG_{inj} (eV)	ΔG_{reg} (eV)
PC1	–0.74	2.18	–1.88	–0.42
PC2	–0.75	2.13	–1.83	–0.43

The E* values were formulated by, $E_{\mathrm{red}}^{*} = E_{\mathrm{Red}} + E_{0\text{-}0}$. $\Delta G_{\mathrm{inj}} = E_{\mathrm{VB}}$ (NiO) – E_{red}^{*} (dye*/dye$^-$) with E_{VB} (NiO) = 0.30 V vs SCE. $\Delta G_{\mathrm{reg}} = E_{\mathrm{Red}}$ (dye/dye$^-$) – E ($I_3^-/I_2^{-\bullet}$) with $E(I_3^-/I_2^{-\bullet})$ = – 0.32 V vs SCE.[11]

Photovoltaic studies

To evaluate the structure-performance relationships of the synthesized dyes, the photoelectrochemical properties of **PC1-2** were determined in NiO-based *p*-DSSCs (see the ESI). The experimentally obtained *J-V* curves of the DSSCs sensitized with dyes **PC1-2** along with the benchmark **P1** dye are depicted in **Figure S17** and the corresponding photovoltaic parameters are summarized in **Table 4**. **Figure 5** shows the *IPCE* spectra of DSSCs

fabricated for all three compounds. From the results, we can notice that the device fabricated with **PC$_1$** shows a higher *PCE* of 0.027 % (J_{SC}: 1.29 mA·cm^{-2}, V_{OC}: 67 mV, and *FF*: 31 %), when compared to the **PC$_2$** (*PCE*: 0.018 %, J_{SC}: 0.92 mA·cm^{-2}, V_{OC}: 68 mV, and *FF*: 30 %) essentially due to a higher J_{SC} for dye **PC$_1$**, whereas the V_{OC} values of both the dyes are found to be almost similar. However, the **P1** benchmark reference is a better performing sensitizer, likely because the ICT involves more clearly the anchoring group (see theoretical calculations). Moreover, the attachment of the dyes by both carboxylic acid and cyano groups certainly forces these new dyes to lay horizontally on NiO surface which consequently accelerates charge recombination and thus explains the lower photovoltaic performances than benchmark **P$_1$** dye. The presence of the dicyano vinylene unit at the extremity of **PC$_1$** most certainly reduces the geminate charge recombination as the electron is moved further awaycompared to **PC$_2$**. This is confirmed by the EDD of **PC$_1$**, which extends towards the electron-withdrawing dicyano vinylene unit (see TD-DFT calculations). Interestingly, the dark current is found to be lower in **PC$_2$**, indicating lower interfacial charge recombination with the electrolyte probably caused by a better shielding of the electrolyte by the dye on the surface of NiO, which can be due to a denser packing on the surface.[44-48] Thus, the probably longer-lived charge-separated state (NiO$^+$/dye$^-$) for **PC$_1$** is likely balanced by the higher charge recombination, explaining the similar V_{OC} with **PC$_2$**. From the results, it can be concluded that the organization of the dye on the NiO surface can be influenced by minor structural alterations.

PC$_1$ displays an improved *IPCE* spectrum compared to that of **PC$_2$**, particularly between 450-550 nm owing to its stronger charge transfer band and explaining its higher short circuit photocurrent density. In short, **PC$_1$** displays superior efficiency owing to the presence of a secondary electron acceptor that enhances the charge transfer band and probably retards geminate charge recombination with the hole in the NiO valence band.

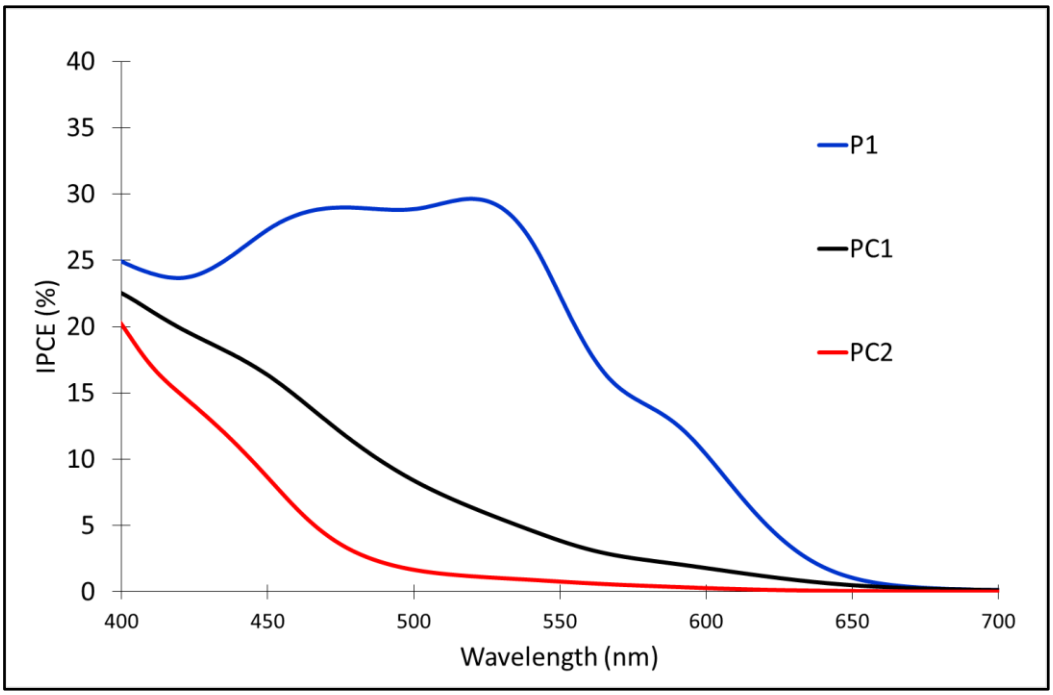

Figure 5. *IPCE* spectra of DSSCs sensitized with dyes **PC1-2** recorded under short-circuit conditions.

Table 4. Photovoltaic performance data of devices sensitized with *p*-type dyes (**PC1-2**) recorded under AM 1.5 (1000 W/m^2).

Sensitizer	J_{SC} **(mA·cm^{-2})**	V_{OC} **(mV)**	***FF* (%)**	***PCE* (%)**
P1	3.55 ± 0.2	115 ± 10	31 ± 3	0.126 ± 0.06
PC1	1.29 ± 0.1	67 ± 5	31 ± 1	0.027 ± 0.01
PC2	0.92 ± 0.1	68 ± 5	30 ± 1	0.018 ± 0.01

Conclusions

In short, we designed and synthesized two new push-pull configured carbazole-based organic chromophores **PC1-2** for *p*-DSSC applications. To probe the "structure-performance" relationships, we have investigated the impact of auxiliary acceptor units as well as end-capping acceptor units on the overall performance of the solar cells. Amongst the fabricated dyes **PC1-2**, the dye carrying malononitrile (**PC1**) as a second electron acceptor displayed the highest *PCE* of 0.027 % (J_{SC}: 1.29 mA·cm^{-2}, V_{OC}: 67 mV, and *FF*: 31 %), when compared to the other dye **PC2** bearing a single auxiliary acceptor unit (*PCE*: 0.018 %). The superiority of **PC1** can be assigned to the presence of a strong end-capping acceptor unit along with the

extended π-conjugation which promotes hole injection and most probably retards charge recombination. Altogether, this study shows that the molecular design of double acceptor sensitizers of the form of D-A-π-A' is a fruitful strategy to make better performing NiO sensitizers. However, if none of the two dyes, outperforms the reference **P1** dye, this is likely due to the more favourable participation of the anchoring unit in that benchmark compound and its mode of binding to NiO with carboxylic acid only, while dyes **PC1** and **PC2** bind with both extremities (CO_2H and CN) that promotes higher charge recombination. This si different to P1, whose cyano stretching band is not affected after binding. Future NiO sensitizer designs with carbazole group should take into consideration this feature. It has been also demonstrated that the slight chemical modification in the design strategy significantly influences the optical, thermal, electrochemical, and photoelectrochemical properties. Thus, we believe that this work contributes to paving the way to a better molecular design strategy of organic chromophores to further ameliorate *p*-type DSSC/tandem DSSC performance.

Supporting Information

The supporting information contains materials and methods, synthetic methods, structural characterization, procedure for calculation of molar extinction coefficient, cyclic voltammograms of **PC1-2**, device fabrication procedures, current density-voltage plots, and theoretical methods.

Acknowledgments

The authors are thankful to NITK, Surathkal, India, for providing necessary laboratory facilities. The authors are also indebted to the CCIPL/GLICID computational centre installed in Nantes for the very generous allocation of computational resources. DJ is indebted to Dr. Patricia Guevara-Level for preliminary calculations. We also thank Conseil Régional des Pays de la Loire and ANR for Financial support *via* LUMOMAT and EUR LUMOMAT Project.

Declaration of Competing Interest

The authors declare that they have no known competing financial interests or personal relationships that could have appeared to influence the work reported in this paper.

References

[1] O'Regan, B.; Grätzel, M. A Low-Cost, High-Efficiency Solar Cell Based on Dye-Sensitized Colloidal TiO_2 Films. *Nature* **1991**, *353*, 737-740.

[2] Hagfeldt, A.; Boschloo, G.; Sun, L.; Kloo, L.; Pettersson, H., Dye-Sensitized Solar Cells. *Chemical Reviews* **2010**, *110*, 6595-6663.

[3] Ye, M.; Wen, X.; Wang, M.; Iocozzia, J.; Zhang, N.; Lin, C.; Lin, Z., Recent Advances in Dye-Sensitized Solar Cells: From Photoanodes, Sensitizers and Electrolytes to Counter Electrodes. *Mater. Today* **2015**, *18*, 155-162.

[4] Nattestad, A.; Mozer, A. J.; Fischer, M. K.; Cheng, Y.-B.; Mishra, A.; Bäuerle, P.; Bach, U., Highly Efficient Photocathodes for Dye-Sensitized Tandem Solar Cells. *Nature Mater.* **2010**, *9*, 31-35.

[5] Odobel, F.; Pellegrin, Y.; Gibson, E. A.; Hagfeldt, A.; Smeigh, A. L.; Hammarström, L., Recent Advances and Future Directions to Optimize the Performances of *p*-Type Dye-Sensitized Solar Cells. *Coord. Chem. Rev*. **2012**, *256*, 2414-2423.

[6] Morandeira, A.; Fortage, J.; Edvinsson, T.; Pleux, L. L.; Blart, E.; Boschloo, G.; Hagfeldt, A.; Hammarström, L.; Odobel, F. Improved photon-to-current conversion efficiency with a nanoporous *p*-type NiO electrode by the use of a sensitizer-acceptor dyad. *J. Phys. Chem. C* **2008**, *112*, 5, 1721–1728.

[7] Powar, S.; Bhargava, R.; Daeneke, T.; Götz, G.; Bäuerle, P.; Geiger, T.; Kuster, S.; Nüesch, F. A.; Spiccia, L.; Bach, U., Thiolate/Disulfide Based Electrolytes for *p*-Type and Tandem Dye-Sensitized Solar Cells. *Electrochim. Acta* **2015**, *182*, 458-463.

[8] Barbero, N.; Magistris, C.; Park, J.; Saccone, D.; Quagliotto, P.; Buscaino, R.; Medana, C.; Barolo, C.; Viscardi, G. Microwave-assisted synthesis of near-infrared fluorescent indole-based squaraines. *Org. Lett.* **2015**, *17*, 3306–3309.

[9] Nattestad, A.; Mozer, A. J.; Fischer, M. K. R.; Cheng, Y. B.; Mishra, A.; Baeuerle, P.; Bach, U. "Highly efficient photocathodes for dye-sensitized tandem solar cells." *Nature Mater.*, **2010**, *9*, 1, 31-35.

[10] Odobel, F.; Le Pleux, L.; Pellegrin, Y.; Blart, E. New photovoltaic devices based on the sensitization of *p*-type semiconductors: challenges and opportunities. *Acc. Chem. Res.* **2010**, *43*, 1063–1071.

[11] Farré, Y.; Maschietto, F.; Föhlinger, J.; Wykes, M.; Planchat, A.; Pellegrin, Y.; Blart, E.; Hammarström, L.; Odobel, F. A Comparative Investigation of the Role of the Anchoring Group on Perylene Monoimide Dyes in NiO-Based Dye-Sensitized Solar Cells. *ChemSusChem* **2020**, *13*, 1844–1855.

[12] Farré, Y.; Raissi, M.; Fihey, A.; Pellegrin, Y.; Blart, E.; Jacquemin, D.; Odobel, F. A Blue Diketopyrrolopyrrole Sensitizer with High Efficiency in Nickel-Oxide-based Dye-Sensitized Solar Cells. *ChemSusChem* **2017**, *10*, 2618–2625.

[13] He, J.; Lindström, H.; Hagfeldt, A.; Lindquist, S.E. Dye-sensitized nanostructured *p*-type nickel oxide film as a photocathode for a solar cell. *J. Phys. Chem. B* **1999**, *103*, 8940–8943.

[14] Shockley, W.; Queisser, H. J. "Detailed Balance Limit of Efficiency of *p-n* Junction Solar Cells". *J. App. Phy.* **1961**, *32* (3): 510–519.

[15] Farré, Y.; Zhang, L.; Pellegrin, Y.; Planchat, A.; Blart, E.; Boujtita, M.; Hammarström, L.; Jacquemin, D.; Odobel, F. Second Generation of Diketopyrrolopyrrole Dyes for NiO-Based Dye-Sensitized Solar Cells. *J. Phys. Chem. C* **2016**, *120*, 7923–7940.

[16] Li, L.; Gibson, E.A.; Qin, P.; Boschloo, G.; Gorlov, M.; Hagfeldt, A.; Sun, L. Double-layered NiO photocathodes for *p*-type DSSCs with record IPCE. *Adv. Mater*. **2010**, *22*, 1759-1762.

[17] Farré, Y.; Raissi, M.; Fihey, A.; Pellegrin, Y.; Blart, E.; Jacquemin, D.; Odobel, F. Synthesis and properties of new benzothiadiazole-based push-pull dyes for *p*-type dye-sensitized solar cells. *Dyes Pigments* **2018**, *148*, 154–166.

[18] Qin, P.; Zhu, H.; Edvinsson, T.; Boschloo, G.; Hagfeldt, A.; Sun, L., Design of an Organic Chromophore for *p*-Type Dye-Sensitized Solar Cells. *J. Am. Chem. Soc.* **2008**, *130*, 8570-8571.

[19] Warnan, J.; Pellegrin, Y.; Blart, E.; Zhang, L.; Brown, A.; Hammarström, L.; Jacquemin, D.; Odobel, F. Acetylacetone anchoring group for NiO-based dye-sensitized solar cell. *Dyes Pigments* **2014,** *105*, 174-179.

[20] Odobel, F.; Pellegrin, Y., Recent Advances in the Sensitization of Wide-Band-Gap Nanostructured *p*-Type Semiconductors: Photovoltaic and Photocatalytic Applications. *J. Phys. Chem. Lett.* **2013**, *4*, 2551-2564.

[21] Gibson, E. A. "Dye-sensitized photocathodes for H_2 evolution." *Chem. Soc. Rev*., **2017**, *46*, 20, 6194-6209.

[22] Nikolaou; V..; Charisiadis; A..; Charalambidis; G..; Coutsolelos; A. G.; Odobel, F.; "Recent advances and insights in dye-sensitized NiO photocathodes for photovoltaic devices." *J. Mater. Chem. A* **2017**, *5*, 40, 21077-21113.

[23] Zhang, Q. Q.; Jiang, K. J.; Huang, J. H.; Zhao, C. W.; Zhang, L. P.; Cui, X. P.; Su, M. J.; Yang, L. M.; Song, Y. L.; Zhou, X. Q., A Push-Pull Thienoquinoidal Chromophore for Highly Efficient *p*-Type Dye-Sensitized Solar Cells. *J. Mater. Chem. A* **2015**, *3*, 7695- 7698.

[24] Wu, F.; Zhu, L.; Zhao, S.; Song, Q.; Yang, C., Engineering of Organic Dyes for Highly Efficient *p*-Type Dye-Sensitized Solar Cells. *Dyes Pigments* **2016**, *124*, 93-100.

[25] Pellegrin, Y.; Pleux, L. L.; Blart, E.; Renaud, A.; Chavillon, B.; Szuwarski, N.; Boujtita, M.; Cario, L.; Jobic, S.; Jacquemin, D.; Odobel, F. Ruthenium polypyridine complexes as sensitizers in NiO based *p*-type dye-sensitized solar cells: Effects of the anchoring groups. *J. Photochem. Photobiol. A: Chem.* **2011**, *219*, 235–242.

[26] Ye, H.; Shen, L.; Zhang, S.; Li, X.; Yu, F.; Diao, R.; Hua, Enhanced Photocurrent via π-Bridge Extension of Perylenemonoimide-Based Dyes for *p*-Type Dye-Sensitized Solar Cells and Photoelectrochemical Cells. *J. ACS Omega* **2018**, *3* (10), 14448-14456.

[27] Cui, J.; Lu, J.; Xu, X.; Cao, K.; Wang, Z.; Alemu, G.; Yuang, H.; Shen, Y.; Cheng, Y.; Wang, M. Organic Sensitizers with Pyridine Ring Anchoring Group for *p*-Type Dye-Sensitized Solar Cells. *J. Phys. Chem. C* **2014**, *118*, 30, 16433–16440.

[28] Qin, P.; Wiberg, J.; Gibson, E.; Linder, M.; Li, L.; Brinck, T.; Hagfeldt, A.; Albinsson, B.; Sun, L. Synthesis and Mechanistic Studies of Organic Chromophores with Different Energy Levels for *p*-Type Dye-Sensitized Solar Cells. *J. Phys. Chem. C* **2010,** *114*, 10, 4738–4748.

[29] Wang, J.; Chen, Y.; Li, F.; Zong, X.; Guo, J.; Sun Z.; Xue S. A new carbazole-based hole-transporting material with low dopant content for perovskite solar cells. *Electrochim. Acta* **2016**, *210*, 673–680.

[30] Yang, S.; Fu, W.; Zhang, Z.; Chen, H.; Li, C. Z. Recent advances in perovskite solar cells: efficiency, stability and lead free perovskite. *J. Mater. Chem.* A **2017** *5*, 11462.

[31] Naik, P.; Planchat, A.; Pellegrin, Y.; Odobel, F.; Adhikari, A. V. Exploring the application of new carbazole based dyes as effective *p*-type photosensitizers in dye-sensitized solar cells. *Sol. Energy* **2017**, *157*, 1064–1073.

[32] Fan, W.; Chang, Y.; Zhao, J.; Xu, Z.; Tan, D. A theoretical study of fused thiophene modified anthracene-based organic dyes for dye-sensitized solar cell applications. *New J. Chem.*, **2018**, *42*, 20163-20170.
[33] Veronese, L.; Procopio, E. Q.; Moehl, T.; Hagfeldt, A. Triarylamine-based hydrido-carboxylate rhenium(i) complexes as photosensitizers for dye-sensitized solar cells. *Phys.Chem.Chem.Phys.*, **2019**, *21*, 7534-7543.
[34] Almenningen, D. M.; Erring H. E.; Vold, M. F.; Buene, A. F.; Venkatraman, V.; Helge H.; Gautun, O. R. Effect of thiophene-based π-spacers on *N*-arylphenothiazine dyes for dye-sensitized solar cells. *Dyes Pigments* **2021**, *185*, 108951.
[35] Mishra, A.; Fischer, M. K. R,; Bauerle, P. Metal-Free Organic Dyes for Dye-Sensitized Solar Cells: From Structure: Property Relationships to Design Rules. *Angew. Chem.*, **2009**, *48*, 2474-2499.
[36] Park, J. Y.; Jang, B. Y.; Lee, C. H.; Yun, H. J.; Kim, J. H. *RSC Adv.*, **2014**,*4*, 61248-61255.
[37] Yang C.H. ; Liao, S. H.; Sun, Y. K.; Chuang, Y. Y.; Wang, T. L.; Shieh. Y. T.; Lin, W. C. Optimization of Multiple Electron Donor and Acceptor in Carbazole-Triphenylamine-Based Molecules for Application of Dye-Sensitized Solar Cells . *J. Phys. Chem. C* **2010**, *114*, 49, 21786–21794
[38] Sun, Z. D.; Zhao, J. S.; Ayyanar, K.; Ju, X. H.; Xia, Q. Y. Design of high performance p-type sensitizers with pyridinium derivatives as the acceptor by theoretical calculations. *RSC Adv.* **2020**, *10*, 10569–10576.
[39] Keremane, K. S.; Adhikari, A. V. Simple carbazole derivatives with mono/di methoxyphenylacrylonitrile substituents as hole-transporting materials: Performance studies in hybrid perovskite solar cells. *Electrochem. Sci. Adv.* **2021**, *1*, (3) DOI 10.1002/elsa.202000036.
[40] Keremane, K. S.; Rao, R.; Adhikari, A. V. Simple 3,6-disubstituted Carbazoles as Potential Hole Transport Materials: Photophysical, Electrochemical and Theoretical Studies. *Photochem. Photobiol.* **2021**, *97*, 289–300.
[41] Keremane, K. S.; Naik, P.; Adhikari, A. V. Simple Thiophene Based Organic Dyes as Active Photosensitizers for DSSC Application: from Molecular Design to Structure Property Relationship. *J. Nano- Electron. Phys.* **2020**, *12*, DOI 10.21272/JNEP.12(2).02039.
[42] Keremane, K. S.; Abdellah, I. M.; Naik, P.; El-Shafei, A.; Adhikari, A. V. Simple thiophene-bridged D–π–A type chromophores for DSSCs: a comprehensive study of their sensitization and co-sensitization properties. *Phys. Chem. Chem. Phys.* **2020**, *22*, 23169–23184.
[43] Nhon, L.; Taggart, A. D.; Moot, T.; Brennaman, M. K.; Jagadesan, P.; Schanze, K. S.; Cahoon, J. F.; Reynolds, J. R. Organic Chromophores Designed for Hole Injection into Wide-Band-Gap Metal Oxides for Solar Fuel Applications. *Chem. Mater.* **2020**, *32*, 8158–8168.
[44] Hu, K.; Sampaio, R. N.; Schneider, J.; Troian-Gautier, L.; Meyer, G. J. Perspectives on Dye Sensitization of Nanocrystalline Mesoporous Thin Films. *J. Am. Chem. Soc.* **2020**, *142*, 16099–16116.
[45] Pleux, L. L.; Smeigh, A. L.; Gibson, E.; Pellegrin, Y.; Blart, E.; Boschloo, G.; Hagfeldt, A.; Hammarström, L.; Odobel, F. Synthesis, photophysical and photovoltaic investigations of acceptor-functionalized perylene monoimide dyes for nickel oxide p-type dye-sensitized solar cells. *Energy Environ. Sci.* **2011**, *4*, 2075–2084.
[46] Huang, Z.; Natu, G.; Ji, Z.; He, M.; Yu, M.; Wu, Y. Probing the Low Fill Factor of NiO *p*-Type Dye-Sensitized Solar Cells. *J. Phys. Chem. C* **2012**, *116*, 50, 26239–26246.

[47] Borgström, M.; Blart, E.; Boschloo, G.; Mukhtar, E.; Hagfeldt, A.; Hammarstrom, L.; Odobel, F. Sensitized hole injection of phosphorus porphyrin into NiO: toward new photovoltaic devices. *J. Phys. Chem. B* **2005**, *109*, 22928–22934.
[48] Liu, Z.; Li, W.; Topa, S.; Xu, X.; Zeng, X.; Zhao, Z.; Chen, W.; Wang, F.; Cheng, Y. B.; He, H. Modulated Charge Injection in *p*-Type Dye-Sensitized Solar Cells Using Fluorene-Based Light Absorbers. *ACS Appl. Mater. Interfaces* **2014**, *6*, 13, 10614–10622.

TOC Graphic

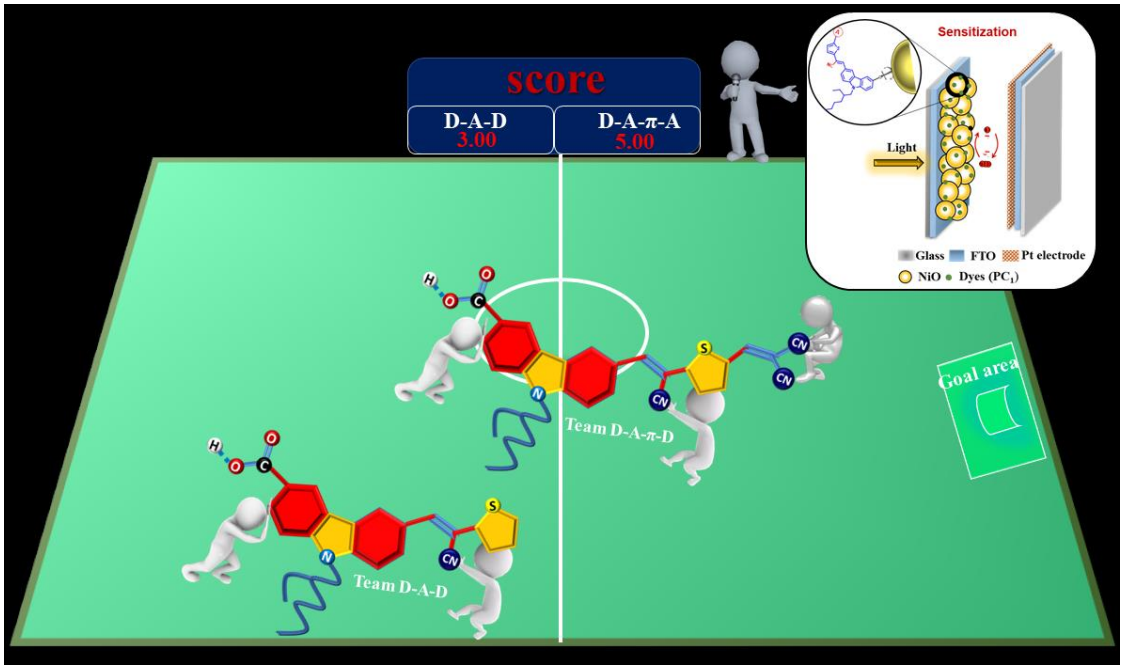
score
D-A-D
3.00
D-A-π-A
5.00
Sensitization
Light
Glass
FTO
Pt electrode
NiO
Dyes (PC1)
Goal area
Team D-A-π-D
Team D-A-D

*****